to B methylenes than A methylenes.

Further information about the polymer chain conformation can be obtained from the ^{13}C chemical shifts of the methine carbons. These chemical shifts show that a hydroxyl substituent in the γ position shifts the methine carbon upfield by less than 2 ppm. It is well-known that the magnitude of the γ effect for a substituent in the trans orientation is different than for that same substituent in the gauche orientation, and this is often referred to as the γ-gauche effect.[27,28] Consequently, the observed chemical shift effect for a substituent in the γ position is dependent upon the relative populations of the t, g$^+$, and g$^-$ conformers. Although a detailed conformational analysis is beyond the scope of this paper, measurement of the methine chemical shift differences provides a starting point for conformational analysis.

Conclusions

This paper illustrates the power of 2D NMR spectroscopy for the analysis of complex copolymers. A combination of homonuclear and heteronuclear 2D NMR spectroscopy was used to make unambiguous comonomer and stereosequence assignments at the triad level in both the ^{1}H and ^{13}C spectra of poly(ethylene-*co*-vinyl alcohol). Methyl end groups were observed and assigned from the 2D COSY spectrum. It was demonstrated that the dominant end groups are methyl groups on terminal ethylene units in –VE sequences, although a low level of methyl ends in –EE sequences also was observed.

Once the assignments were known, the CH/OH coupling constants were measured from the 2D *J*-resolved spectrum. The magnitude of the CH/OH coupling constant is sequence dependent, with all sequences containing meso VV dyads having a smaller coupling constant than other sequences. This indicates that the average dihedral angle between the methine and hydroxyl protons is sequence dependent. The 2D ^{13}C–^{1}H correlated spectrum was used to distinguish equivalent and nonequivalent methylene protons, and this provided further insight into the chain conformation.

Registry No. (E)(VOH) (copolymer), 25067-34-9.

References and Notes

(1) Brown, L. R. *J. Magn. Reson.* **1984**, *57*, 513.
(2) Cheng, H. N.; Lee, G. H. *Polym. Bull.* **1984**, *12*, 463.
(3) Schilling, F. C.; Bovey, F. A.; Bruch, M. D.; Kozlowski, S. A. *Macromolecules* **1985**, *18*, 1418.
(4) Bruch, M. D.; Bovey, R. A.; Cais, R. E. *Macromolecules* **1984**, *17*, 2547.
(5) Cheng, H. N.; Lee, G. H. *Polym. Bull.* **1985**, *13*, 549.
(6) Chang, C.; Muccio, D. D.; St. Pierre, T. *Macromolecules* **1985**, *18*, 2334.
(7) Mirau, P. A.; Bovey, F. A. *Macromolecules* **1986**, *19*, 210.
(8) Bruch, M. D.; Bonesteel, J. K. *Macromolecules* **1986**, *19*, 1622.
(9) Heffner, S. A.; Bovey, F. A.; Verge, L. A.; Mirau, P. A.; Tonelli, A. E. *Macromolecules* **1986**, *19*, 1628.
(10) Crowther, M. W.; Szeverenyi, N. M.; Levy, G. C. *Macromolecules* **1986**, *19*, 1333.
(11) Bruch, M. D.; Payne, W. G. *Macromolecules* **1986**, *19*, 2712.
(12) Macura, S.; Brown, L. R. *J. Magn. Reson.* **1983**, *53*, 529.
(13) Gippert, G. P.; Brown, L. R. *Polym. Bull.* **1984**, *11*, 585.
(14) Bruch, M. D.; Bovey, F. A.; Cais, R. E.; Noggle, J. H. *Macromolecules* **1985**, *18*, 1253.
(15) Bauman, R.; Wider, G.; Ernst, R. R.; Wuethrich, K. *J. Magn. Reson.* **1981**, *44*, 402.
(16) Mersh, J. D.; Sanders, J. K. M. *J. Magn. Reson.* **1982**, *50*, 171.
(17) Nagayama, K.; Kumar, A.; Wuethrich, K.; Ernst, R. R. *J. Magn. Reson.* **1980**, *40*, 321.
(18) Aue, W. P.; Karhan, J.; Ernst, R. R. *J. Chem. Phys.* **1976**, *64*, 4226.
(19) Brownstein, S. *J. Magn. Reson.* **1981**, *42*, 150.
(20) Bendall, M. R.; Pegg, D. T.; Doddrell, D. M. *J. Magn. Reson.* **1981**, *45*, 8.
(21) (a) DeMember, J. R.; Haas, H. C.; MacDonald, R. L. *J. Polym. Sci., Part B* **1972**, *10*, 385. (b) Moritani, T.; Kuruma, I.; Shibatani, S.; Fujiwara, Y. *Macromolecules* **1972**, *5*, 577.
(22) Kumar, A. *J. Magn. Reson.* **1978**, *30*, 227.
(23) Bodenhausen, G.; Freeman, R.; Morris, G. A.; Turner, D. L. *J. Magn. Reson.* **1978**, *31*, 75.
(24) Cheng, H. N.; Lee, G. H. *Macromolecules* **1988**, in press.
(25) Moritani, T.; Iwasaki, H. *Macromolecules* **1978**, *11*, 1251.
(26) Ovenall, D. W. *Macromolecules* **1984**, *17*, 1458.
(27) Tonelli, A. E. *Macromolecules* **1985**, *18*, 1086.
(28) Schilling, F. C.; Tonelli, A. E. *Macromolecules* **1986**, *19*, 1337.

A ^{13}C Nuclear Magnetic Resonance Study of the Triad Sequence Structure of Block and Statistical Copolymers of Ethylene Oxide and Propylene Oxide

Frank Heatley,*[†] Yun-Zhu Luo,[‡] Ji-Feng Ding,[†] Richard H. Mobbs,[†] and Colin Booth[†]

Department of Chemistry, University of Manchester, Manchester M13 9PL, U.K., Department of Chemistry and Materials, National University of Defense Technology, Changsha, Hunan Province, People's Republic of China, and Department of Applied Chemistry, Shenzhen University, Shenzhen, Guangdong Province, People's Republic of China. *Received October 5, 1987*

ABSTRACT: ^{13}C NMR spectra of homopolymers and block and statistical copolymers of ethylene oxide and propylene oxide have been studied in $CDCl_3$ solution at 75.5 MHz by using resolution-enhancement and subspectrum editing techniques. Triad sequences have been unequivocally identified, including the effects of stereoisomerism and end groups and the assignments tested for consistency by using statistical relationships and a simple chemical shift substituent additivity scheme.

Introduction

Statistical and block copolymers of ethylene oxide (EO) and propylene oxide (PO) have numerous applications as surfactants, and the development of characterization methods is of considerable interest. The most powerful method of characterizing the chemical structure is carbon-13 nuclear magnetic resonance (NMR), and in early studies of statistical oxyethylene/oxypropylene (EP) copolymers,[1,2] the monomer sequence was elucidated at the diad level. More recently a triad analysis of 25-MHz ^{13}C spectra has been reported,[3] but this involved computer decomposition of the intensities of strongly overlapping

---

[†] University of Manchester.

[‡] National University of Defense Technology and Shenzhen University.

0024-9297/88/2221-2713$01.50/0

Table I
Molecular Weights of Polymers Studied

sample	$\bar{M}_n$	$\bar{M}_w/\bar{M}_n$
E_{39}	1720	1.09
$P_1E_{39}P_1$	1860	1.09
$P_2E_{39}P_2$	1950	1.09
$P_3E_{39}P_3$	2060	1.09
$P_{10}E_{39}P_{10}$	2900	1.11
P_{26}	1510	1.15
$E_9P_{26}E_9$	2280	1.18
P_{81}	4700	
P_{16}	940	1.05
$E_{0.3}P_{16}E_{0.3}$	970	1.05
P_{28}	1600	1.09
UCONA	13700	1.27
CH-EP	3290	1.17

bands. In view of the advantages in sensitivity and chemical shift resolution gained by using higher magnetic fields, a further study using a high-field spectrometer and recent developments in experimental techniques appeared appropriate. This paper reports an investigation at 75.5 MHz of ^{13}C spectra of statistical and block EP copolymers together with EO and PO homopolymers for comparison. The spectrum interpretation has been assisted considerably by the use of the attached proton test (APT)[4-6] pulse sequence to obtain CH and CH_2 subspectra and of the Lorentz–Gaussian transformation technique[7] for resolution enhancement.

Experimental Section

NMR Spectroscopy. ^{13}C spectra were obtained by using a Varian Associates XL-300 spectrometer operating at 75.5 MHz. Solutions in $CDCl_3$ containing ca. 150 mg of polymer/cm^3 of solvent were used. Chemical shifts were initially referenced to a solvent value of δ_C 76.90. However, fluctuations of up to 0.1 ppm for a given peak were observed depending on chain structure. Spectra were therefore referenced internally by setting either the $E\underline{E}E$ peak to δ_C 70.33 or the *mm* t-$\vec{P}\underline{\vec{P}}\vec{P}$ peak to δ_C 75.26 as found for solutions of the homopolymers. (See the Results and Discussion for an explanation of the notation.)

CH and CH_2 subspectra were obtained by using APT[4-6] pulse sequences. This technique is essentially a spin–echo experiment with a variable interval, τ, between the 90° and 180° pulses. If $\tau = 1/(4J_{CH})$, where J_{CH} is the ^{13}C–^1H coupling constant, all ^{13}C signals are the same sign (say positive) whereas if $\tau = 3/(4J_{CH})$, CH_2 signals are positive and CH signals negative. For the ideal relaxation-free sequence the magnitudes of the signals in the two cases are equal, so that addition of the two spectra gives the CH_2 subspectrum, whereas subtraction gives the CH subspectrum. In practice the spectra were not perfectly balanced, but the mixing required to produce the subspectra was easily found empirically by nulling peaks known to be entirely CH or CH_2. It was found that the $1/(4J_{CH})$ and $3/(4J_{CH})$ spectra with J_{CH} = 140 Hz needed to be added or substracted in the proportions 1:1.1, respectively. In this work the APT technique was preferred to the more widely used DEPT technique[8] because of the lack of computer control of decoupler power. It was not possible to chain standard aquisitions requiring relatively low-power continuous decoupling with DEPT spectra requiring high-power decoupler pulses, during the overnight periods available for this work.

Resolution enhancement was performed by using the Lorentz–Gaussian transformation technique[7] (LGRE) that consists of multiplication of the free induction decay first by an exponential $\exp(+t/T_e)$ and then by a Gaussian function $\exp[-(t/T_g)^2]$.

Materials. Block copoly(oxypropylene/oxyethylene/oxypropylene)s with a central block of 39 oxyethylene units were prepared as described earlier.[9] These are denoted $P_xE_{39}P_x$, and their poly(oxyethylene) precursor E_{39}: see Table I. Other homopolymers and block copolymers were prepared by using the same experimental method as follows.

Propylene oxide (BDH Ltd., 99.5%) was stirred over CaH_2 under dry nitrogen (>24 h). Ethylene oxide (Fluka AG., 99.8%) was passed through a glass tube (400 mm long, 20-mm i.d.) packed with crushed CaH_2. Ethylene glycol (BDH, 99%) was fractionally distilled under reduced pressure (midpoint cut, bp 80–81 °C (3.5 mmHg)). Propylene glycol (BDH, 99%) was stirred over $MgSO_4$ (>48 h) and then fractionally distilled under reduced pressure (midpoint cut, bp 71 °C (12 mmHg)) onto type 4A molecular sieve. 1-Methoxy-2-propanol (Aldrich Ltd., 98%) was stirred over $MgSO_4$ (>24 h) and then fractionally distilled (midpoint cut, bp 119 °C) onto type 4A molecular sieves. Tetrahydrofuran (THF) was stirred over CaH_2 and distilled onto sodium wire plus benzophenone. The deep blue color of the sodium benzophenone complex formed on standing.

A block copoly(oxyethylene/oxypropylene/oxyethylene) with a central block of 26 oxypropylene units (denoted $E_9P_{26}E_9$) and its poly(oxypropylene) precursor (P_{26}) were prepared in glass apparatus at atmospheric pressure. The reaction temperature was generally kept below 50 °C, and a crown ether was added in order to increase the reaction rate. KOH (M&B, 0.299 g, 15% wt H_2O, 0.0045 mol of KOH, 0.0025 mol of H_2O), additional initiator ($HOCH_2CH_2OH$, 0.080 g, 0.0013 mol), and 18-crown-6 (1.197 g, 0.0045 mol) were mixed in the reaction vessel at 50 °C. Propylene oxide (16.6 g, 0.286 mol) was added dropwise, so that the internal temperature was maintained at ca. 50 °C, over a total period of 10 h. After removal of excess propylene oxide (ca. 3 g) a sample of homopoly(oxypropylene) was removed. Ethylene oxide (ca. 5 g) was then added dropwise to the reaction flask and the block copolymer formed (50–70 °C, 3 h). Crown ether and catalyst residues were removed from both products by stirring a sample of each for 3 h with an equal volume of dilute hydrochloric acid (excess), extracting with dichloromethane, water washing the extracts, and then evaporating the organic layer. Finally the polymers were pumped to complete dryness ($<10^{-3}$ mmHg, >24 h). The same method was used to prepare a sample of poly(oxypropylene) of higher molecular weight (P_{81}).

A second sample of block copoly(oxyethylene/oxypropylene/oxyethylene) with a central-block length of 16 P units and much shorter end blocks (ca. 0.3 E unit) was prepared by using a thick-walled Pyrex ampule sealed by a PTFE tap. Dry propylene glycol (3 cm^3) was diluted with pure THF (5 cm^3) and reacted under nitrogen with potassium metal (0.382 g, 0.0098 mol). The resulting solution was quantitatively transferred to the ampule which was evacuated to remove solvent and some propylene glycol giving a residue of the potassium salt/propylene glycol mixture (1.58 g, equivalent to 0.016 mol of propylene glycol). Propylene oxide (15.88 g, 0.273 mol) was added by vacuum transfer, and the sealed ampule was held at 80 °C for 3 days. After evacuation to remove excess monomer, a small sample of the homopoly(oxypropylene) was removed. Ethylene oxide (ca. 0.9 g) was then added and the block copolymer formed (80 °C, 22 h). Catalyst residues were removed from the two products by stirring a sample of each with an equal volume of dilute hydrochloric acid (excess) for 24 h and then extracting with an equal volume of pentane. The pentane layer was washed twice with equal volumes of 2.2 M aqueous potassium chloride solution and then with an equal volume of water. The pentane was evaporated off in vacuum and the residual polymer thoroughly dried ($<10^{-3}$ mHg, >24 h).

Finally a sample of poly(oxypropylene) was prepared in an ampule by use of 1-methoxy-2-propanol as initiator. The initiator (4.61 g) was reacted with metallic K (0.66 g) under nitrogen, and a sample of this solution (0.80 g, 0.0078 mol of initiator) was placed in the dry ampule. Propylene oxide (ca. 11 g) was added by vacuum transfer, and the sealed ampule was held at 80 °C for 4 days. The sample (designated P_{28}) was purified by the method described above.

Average molecular weights ($\bar{M}_n$) of the homopolymers were determined by GPC in comparison with poly(oxypropylene) or poly(oxyethylene) standards, while those of the block copolymers were calculated from the $\bar{M}_n$ of their homopolymer precursors making use of the compositions determined by ^1H NMR (300 MHz, 5–10 wt % solutions in $CDCl_3$) from the ratios of integrals of the CH_3 and CH/CH_2 regions. Molecular weight ratios ($\bar{M}_w/\bar{M}_n$) were determined directly from the calibrations for all samples. Note that the fact that about one-fifth by number of the P_{26} chains were initiated by ethylene glycol was ignored in the calculation of composition.

Samples of stat copoly(oxyethylene/oxypropylene) were obtained from commercial sources, one from Union Carbide Ltd.

(sample UCONA) and a second from a Chinese source (sample CH-EP).

Table I summarizes molecular weight data for all samples.

Results and Discussion

To specify a particular carbon concisely, the following notation has been adopted: (i) Ethylene oxide units are designated by E and propylene oxide by $\vec{P}$, the arrow running from the CH_2 tail (T) to the $CH(CH_3)$ head (H). (ii) The unit in which the carbon in question is located is indicated by underlining. Within a P unit, the symbols t, s, and p distinguish the CH, CH_2, and CH_3 carbons, respectively. If an E unit is at the center of a symmetrical sequence, the carbons are identical and hence no distinction is necessary. If the sequence is unsymmetrical, the E CH_2s are not identical, and in this case the CH_2s are designated by a or b representing respectively the left- or right-hand CH_2 in the sequence as written. (iii) An end unit is designated by an asterisk. (iv) Isotactic PP diads are designated *m* and syndiotactic *r*. The fraction of a particular sequence is denoted by, e.g., (EE$\vec{P}$), and includes the reverse sequence if unsymmetrical.

The main-chain CH and CH_2 resonances were found to be the most sensitive to chain stereochemistry and sequence structure, and the following discussion is concentrated on this region. The methyl resonances were much less informative and are only briefly discussed.

NMR Spectra of Homopolymers. In analyzing the copolymer spectra it is helpful to consider the homopolymer spectra. Although detailed reports of the ^{13}C spectra of poly(ethylene oxide)[10] and poly(propylene oxide)[11-14] have been published, the solvents and concentrations used differed from this work. Furthermore the resonance frequency in this work was significantly higher than in earlier studies with consequent increase in sensitivity and chemical shift resolution. It is therefore worthwhile describing the homopolymer spectra in detail before considering the copolymers.

Poly(ethylene oxide) (PEO). The sample studied, E_{39}, was hydroxy-terminated, and in addition to the main-chain resonance at δ_C 70.33, three terminal carbons were observed at δ_C 61.46 (b-$\underline{E}$*), 72.35 (a-$\underline{E}$*), and 70.09 δ_C (b-$\underline{E}$E*). This assignment is consistent with that of Holmes and Moniz[10] and with empirical substituent parameters for linear alkanes.[15]

Poly(propylene oxide) (PPO). The main peaks in all PPO samples studied here were similar to those of essentially H–T atactic PPO published previously,[11,12,14] though because of our higher frequency, greater discrimination of longer stereosequences was achieved, particularly with the aid of resolution enhancement as shown for sample P_{26} in Figure 1a. The stereochemical assignment follows ref 12. Novel splittings revealed here are the resolution of the center t-$\vec{P}\underline{\vec{P}}\vec{P}$ resonance into distinct peaks for *mr* and *rm* triads and resolution of the *r* s-$\vec{P}\underline{\vec{P}}$ peak into tetrads. The uniform intensity distribution over the triad and tetrad peaks indicates an essentially random stereosequence distribution.

In addition to the major peaks, a number of minor peaks are also observed, arising from end groups, inverted monomers, and initiation sites. Peaks from inverted units are distinguishable from the other two by an intensity which is independent of molecular weight, while peaks from initiators can be identified by changing the initiator structure. Some of these peaks are clearly separated from the major peaks, but others are obscured and are revealed only by the APT procedure. Figures 1–3 show several expanded traces and subspectra illustrating spectral features leading to the peak assignments in Table II. Points of interest are as follows: (i) The CHOH/CH_2OH region, illustrated by that of sample P_{26} in Figure 1b, showed t-$\underline{\vec{P}}$* signals only, with no evidence of CH_2OH end groups expected at δ_C 65–67. This is consistent with predominantly

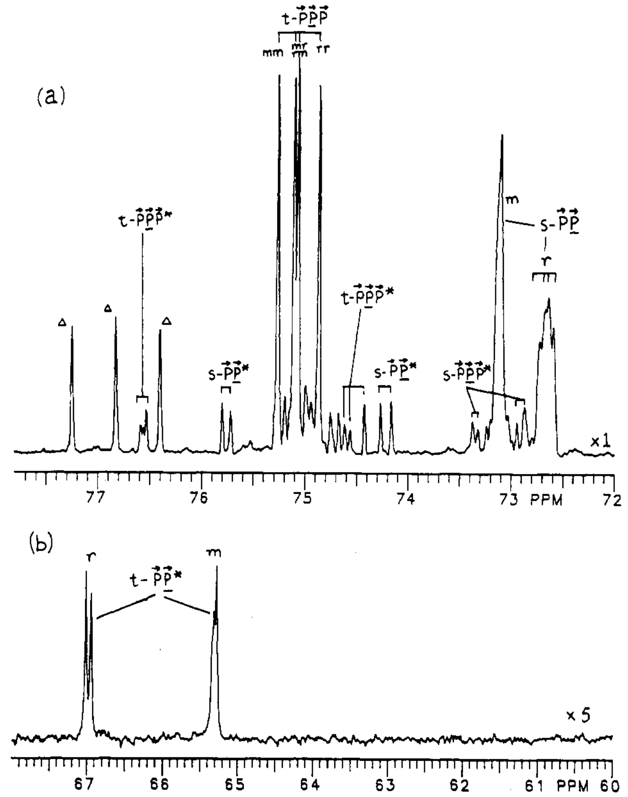

Figure 1. ^{13}C spectra of P_{26}: (a) main-chain resonances, resolution-enhanced with T_e = 0.2 and T_g = 0.3 s; (b) terminal carbon resonances (Δ, $CDCl_3$ solvent).

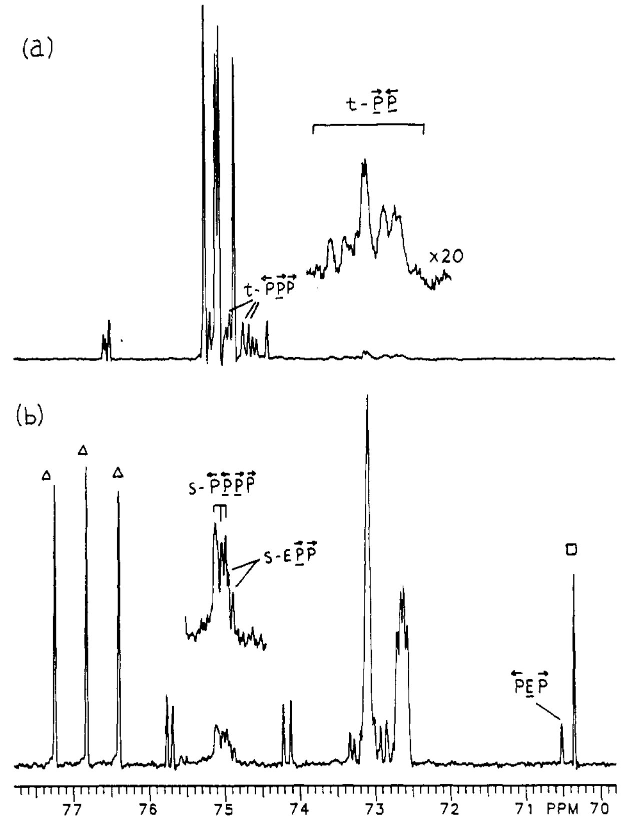

Figure 2. Resolution-enhanced (T_e = 0.2, T_g = 0.3 s) subspectra of P_{26}: (a) CH, (b) CH_2 carbons (Δ, $CDCl_3$ solvent; □, residual crown ether).

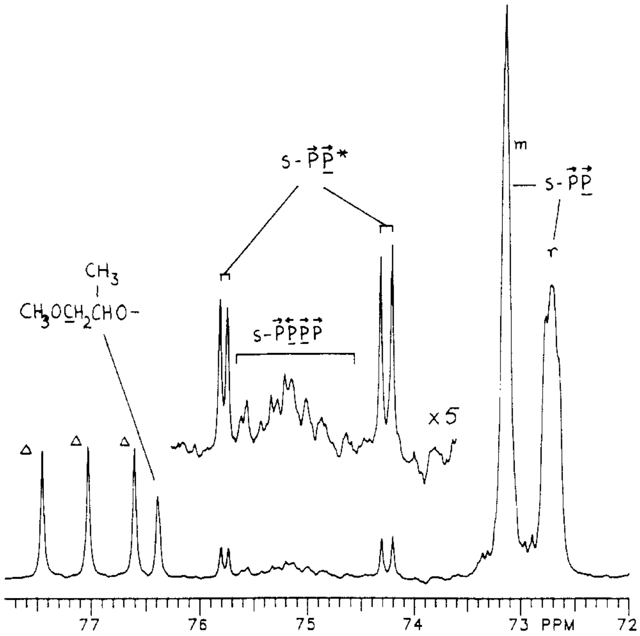

Figure 3. CH_2 subspectrum of P_{26} (△, $CDCl_3$ solvent).

regular H→T addition proceeding in both directions from a bifunctional initiator, giving CH(OH) ends only. (ii) Several other resonances associated with chain ends are observed in the vicinity of the main-chain resonances as shown in Figure 1. The assignments given were achieved by comparing the spectra of samples of different molecular weight and by comparing with the spectra of PEP triblock copolymers described below. Schilling and Tonelli[14] using C_6D_6 solvent also identified end-group signals at frequencies similar to those reported here, but no assignment was made. It is noticeable that the stereochemistry of the terminal diad induces a much larger splitting of the t-$\vec{P}\underline{\vec{P}}$*, s-$\vec{P}\underline{\vec{P}}$*, and t-$\vec{P}\underline{\vec{P}}\vec{P}$* resonances than the stereochemistry of the internal diads does for the resonances of the internal carbons. (iii) The spectrum of sample P_{26}, prepared with ethylene glycol (EG) in the initiator, shows a small CH_2 peak in the PEO region at δ_C 70.50 (see Figure 2b). Comparison of the intensities of this peak in the spectra of samples P_{26} and P_{81} showed that it is attributable to $\overleftarrow{P}\underline{E}\vec{P}$ initiation sites. For sample P_{26} its intensity is only about one-fifth of the total terminal CHOH intensity indicating that only about one-fifth of the chains were initiated by EG. The remaining chains were initiated by water or hydroxyl, first producing propylene glycol which then propagates in both directions giving a symmetrical $\overleftarrow{P}\vec{P}$ initiation site. According to calculations of the γ-gauche effect on ^{13}C chemical shifts in PPO using the rotational isomeric state model[14] and also according to a qualitative consideration of the effect of neighboring methyl groups[7] (see below), s-$\overleftarrow{P}\underline{\overleftarrow{P}\vec{P}}\vec{P}$ and s-$E\underline{\vec{P}}\vec{P}$ resonances should occur in the major t-$\vec{P}\underline{\vec{P}}\vec{P}$ region. Such "hidden" peaks are indeed revealed in the CH_2 subspectrum in Figure 2b. These "hidden" CH_2 peaks have been assigned to $\overleftarrow{P}\overleftarrow{P}\vec{P}\vec{P}$ and $E\vec{P}\vec{P}$ sequences by comparison with spectra of PPO and PEP triblock copolymers (see below) prepared in the absence of EG. The total intensity of the resonances from these initiation sites matches that from the end groups and decreases with increasing molecular weight. (iv) Inverted addition of a PO monomer will produce $\vec{P}\overleftarrow{P}$ and $\overleftarrow{P}\vec{P}$ diads during propagation. Chemical shift calculations[1,14] place peaks from t-$\underline{\vec{P}\overleftarrow{P}}$ carbons in the region of the main CH_2 resonances, and the CH subspectrum in Figure 2a shows a number of such peaks in the range δ_C 72.5–73.8. Given the strong tendency of the PPO in anionic polymerization to propagate by H→T addition, it would be expected that the occasional H→H addition is immediately followed by a T→T addition, giving a $\vec{P}\vec{P}\overleftarrow{P}\vec{P}$ sequence. Here the two CH carbons in the $\vec{P}\overleftarrow{P}$ diad are not identical, and if each is sensitive to the $\vec{P}\vec{P}\overleftarrow{P}\vec{P}$ tetrad stereochemistry, a total of 16 distinct peaks should be observed. Substantial overlap amongst this large number of resonances would account for the rather poorly resolved spectrum actually observed for the t-$\underline{\vec{P}\overleftarrow{P}}$ resonances. Likewise, the s-$\underline{\overleftarrow{P}\vec{P}}$ carbons are not identical when this diad arises from monomer inversion rather than from an initiation site. In the spectrum illustrated in Figure 2, propagation s-$\underline{\overleftarrow{P}\vec{P}}$ peaks are obscured by the much more intense initiation s-$\underline{\overleftarrow{P}\vec{P}}$ peaks. However, the propagation s-$\underline{\overleftarrow{P}\vec{P}}$ pattern is clearly revealed in Figure 3, which shows the CH_2 subspectrum of a PPO sample, P_{28}, initiated by the monofunctional initiator $CH_3OCH(CH_3)CH_2OH$, and hence lacking $\overleftarrow{P}\vec{P}$ initiation diads. Numerous peaks are observed in the range δ_C 74.5–75.6 with total intensity equal (within experimental error) to that of the t-$\underline{\vec{P}\overleftarrow{P}}$ resonances. The total intensity from t-$\underline{\vec{P}\overleftarrow{P}}$ carbons amounted to 5% of the total CH intensity, corresponding to 2.5% of units being inverted. The terminal methoxyl resonance of this sample occurred as a single line at δ_C 58.76.

NMR Spectra of Copolymers. PEP Triblock Copolymers. These samples proved particularly useful in furnishing assignments for oxypropylene end groups and

Table II
^{13}C Chemical Shift Assignments for E/P Polymers in $CDCl_3$ at 22 °C and Concentration of 0.15 g cm^{-3}

carbon	δ_C
$E\underline{E}E$, a-$E\underline{E}\vec{P}$	70.33
b-$E\underline{E}\vec{P}$, $\overleftarrow{P}\underline{E}\vec{P}$	70.50
b-$\vec{P}\underline{E}E$	70.60
a-$E\vec{P}\underline{E}E$, a-$E\vec{P}\underline{E}\vec{P}$	68.29
a-$\vec{P}\vec{P}\underline{E}E$, a-$\vec{P}\vec{P}\underline{E}\vec{P}$	68.29, 68.37
b-$\vec{P}\underline{E}\vec{P}$	70.74
$\vec{P}\underline{E}\overleftarrow{P}$	68.50
s-$\vec{P}\underline{\vec{P}}$	72.64, 73.11
t-$\vec{P}\underline{\vec{P}}\vec{P}$	74.86, 75.06, 75.10, 75.26
s-$\overleftarrow{P}\underline{\overleftarrow{P}\vec{P}}\vec{P}$	75.00, 75.03, 75.11
s-$\vec{P}\underline{\overleftarrow{P}\vec{P}}$	74.5–75.5
t-$\underline{\vec{P}\overleftarrow{P}}\vec{P}$	72.5–73.8
t-$\vec{P}\underline{\vec{P}}E$	74.89, 75.06
s-$E\underline{\vec{P}}\vec{P}$	74.87, 74.91
t-$E\underline{\vec{P}}\vec{P}$	74.73, 74.94
t-$E\underline{\vec{P}}\overleftarrow{P}$	72.75, 73.12
s-$E\underline{\vec{P}}E$	74.91
t-$E\underline{\vec{P}}E$	74.73
b-$EE\underline{E}$*	61.46
a-$EE\underline{E}$*	72.35
b-$E\underline{E}E$*	70.09
b-$\vec{P}E\underline{E}$*	61.48
a-$\vec{P}E\underline{E}$*	72.29
b-$\vec{P}\underline{E}E$*	70.51
a-$\vec{P}\underline{E}E$*	68.42, 68.45
b-$E\vec{P}\underline{E}$*	61.72
b-$\vec{P}\vec{P}\underline{E}$*	61.72, 61.83
a-$\vec{P}\vec{P}\underline{E}$*	70.46, 70.51
t-$\vec{P}\vec{P}\underline{\vec{P}}$*	65.32, 66.95, 67.03
s-$\vec{P}\vec{P}\underline{\vec{P}}$*	74.16, 74.26, 75.71, 75.79
t-$\vec{P}\underline{\vec{P}}\vec{P}$*	74.42, 74.56, 74.61, 76.53
s-$\vec{P}\underline{\vec{P}}\vec{P}$*	72.86, 73.04, 73.32, 73.36
t-$E\vec{P}\underline{\vec{P}}$*	65.48, 66.85
s-$E\vec{P}\underline{\vec{P}}$*	74.28, 75.53
t-$E\underline{\vec{P}}\vec{P}$*	74.24, 75.88
s-$E\underline{\vec{P}}\vec{P}$*	75.01, 75.10
t-$\vec{P}E\underline{\vec{P}}$*, t-$EE\underline{\vec{P}}$*	65.98
s-$EE\underline{\vec{P}}$*	76.76

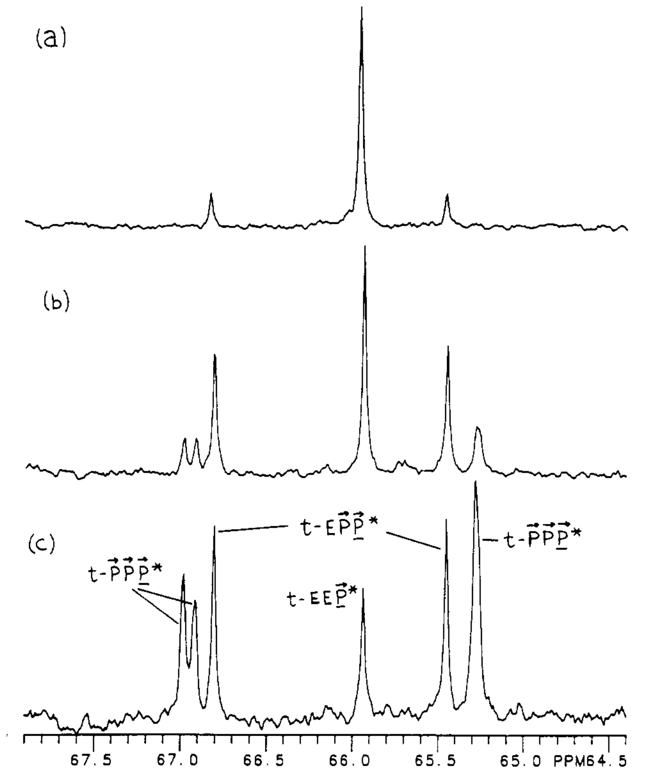

Figure 4. CHOH terminal resonances of PEP triblock copolymers: (a) $P_1E_{39}P_1$, (b) $P_2E_{39}P_2$, (c) $P_3E_{39}P_3$.

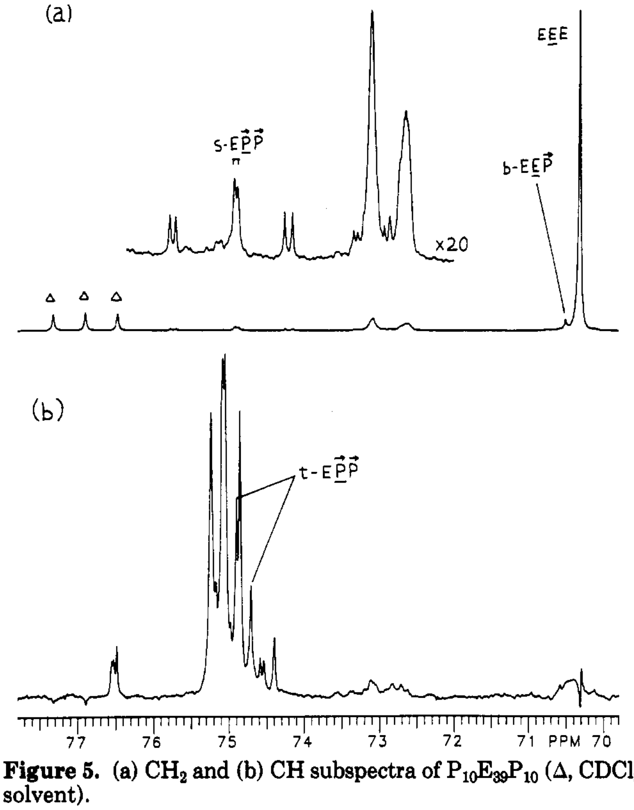

Figure 5. (a) CH_2 and (b) CH subspectra of $P_{10}E_{39}P_{10}$ (Δ, $CDCl_3$ solvent).

$E\vec{P}$ sequences. Figure 4 shows the terminal CHOH region of spectra of samples with different P block lengths, while Figure 5 shows the main backbone carbon region. From the variation in relative intensities in Figure 4, it is a straightforward task to identify resonances corresponding to oxyethylene chains terminated by one, two, or three or more P units. For chains terminated by a single P unit, there is of course no stereochemical splitting, whereas with two P units, there is a large splitting due to *m*/*r* isomerism of the terminal diad. With three or more P units, the terminal carbon resonance is identical with that of PPO homopolymer. Peaks from penultimate units occur in the vicinity of main-chain carbons and were distinguished in the same way as peaks from the end units. These assignments are given in Table II. The exceptional high-frequency shift of the s-$E\underline{\vec{P}}^*$ carbon is noteworthy.

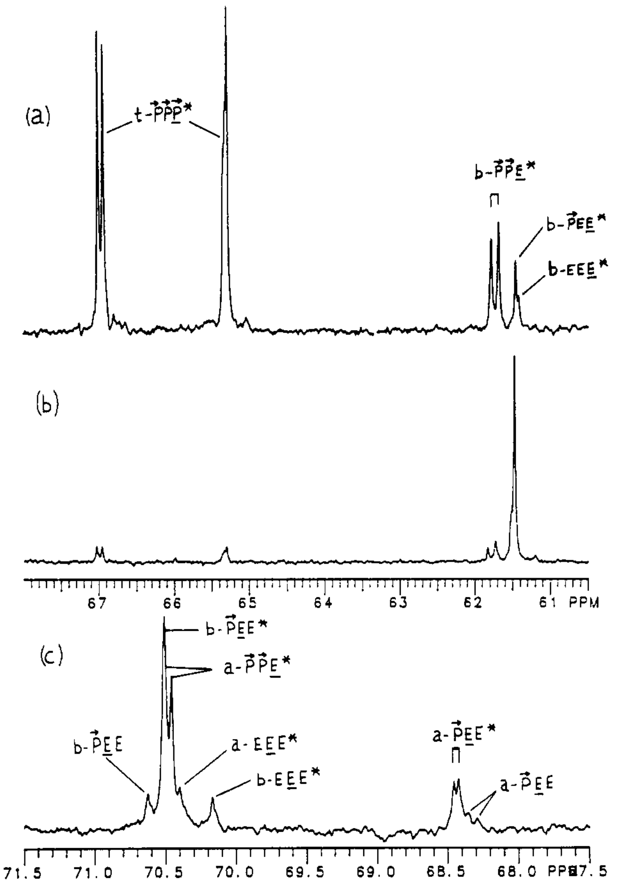

Figure 6. ^{13}C spectra of EPE triblock copolymers: (a) terminal resonances of $E_{0.3}P_{16}E_{0.3}$, (b) terminal resonances of $E_9P_{26}E_9$, (c) end-group resonances of $E_{0.3}P_{26}E_{0.3}$ in vicinity of PEO resonance.

The main-chain spectrum of sample $P_{10}E_{39}P_{10}$ illustrated in Figure 5 shows three features of significance for the analysis of the spectra of the statistical copolymers. The similarity of the major peaks to those of PEO and PPO homopolymers is apparent. The major difference is the occurrence in the triblock copolymer of additional peaks arising from $E\vec{P}$ junctions. (Note that from the method of preparation, both block junctions are of this form.) Additional CH peaks are found at δ_C 74.73 and 74.94, attributable to t-$E\underline{\vec{P}}P$ carbons split by stereoisomerism. Two CH_2 peaks characteristic of the junction are also observed. The s-$E\underline{\vec{P}}\vec{P}$ resonance is hidden by the resonances of the main-chain CH carbons but is revealed in the CH_2 subspectrum (Figure 5a); this resonances matches the s-$E\underline{\vec{P}}\vec{P}$ resonance in EG-initiated PPO discussed above. The other junction CH_2 is the b-$E\underline{E}\vec{P}$ carbon which gives rise to a small peak to the high-frequency side of the intense $E\underline{E}E$ peak. The b-$E\underline{E}\vec{P}$ carbon has the same chemical shift as the $\overleftarrow{P}\underline{E}\vec{P}$ carbon found in the EG-initiated PPO.

EPE Triblock Copolymer. The PPO central block from which these polymers are formed has the structure elucidated above for PPO homopolymer; i.e., the triblock structure is properly written $E_n(\overleftarrow{P})_m(\vec{P})_mE_n$. Thus both block junctions are of the form $\vec{P}E$.

Parts a and b of Figure 6 show spectra of the terminal

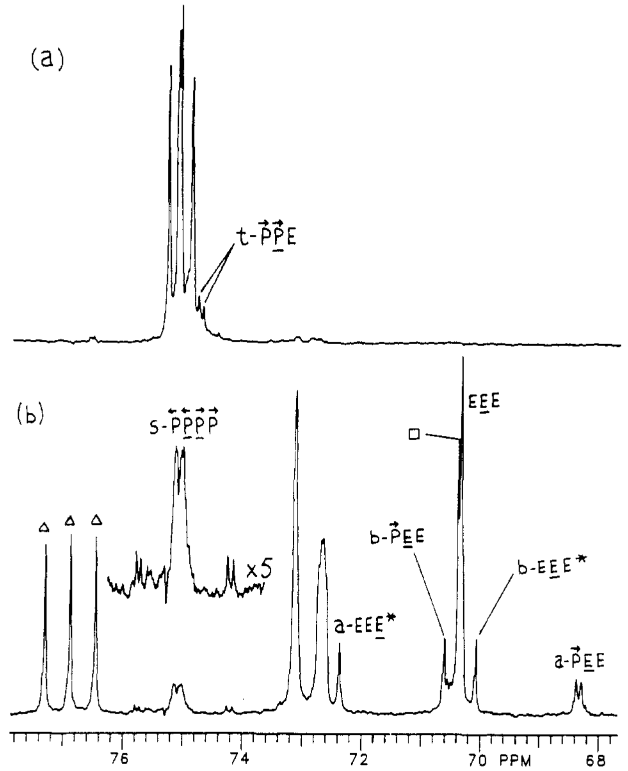

Figure 7. (a) CH and (b) CH_2 subspectra of $E_9P_{26}E_9$ (Δ, $CDCl_3$ solvent; □, residual crown ether).

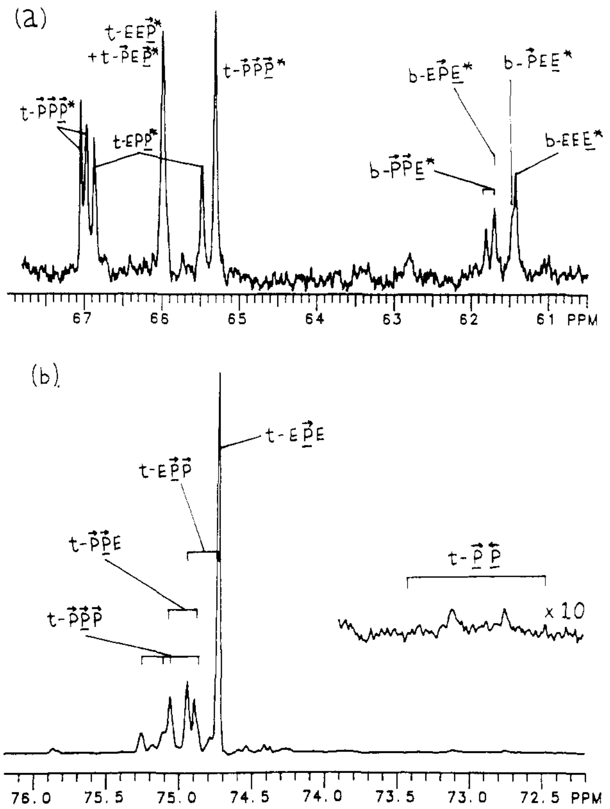

Figure 8. Spectra of low MW statistical EP copolymer, CH-EP: (a) terminal resonances, (b) CH subspectrum of main-chain carbons, resolution-enhanced with $T_e = 0.2$ and $T_g = 0.3$ s.

carbon region for two samples with different E-block lengths (*n*). The various terminal CH_2OH peaks can be readily assigned by the variation in intensity with *n* and also by comparison with the chemical shift of CH_2OH in PEO homopolymer. Small splittings due to stereoisomerism in $\vec{P}\vec{P}$ diads are apparent in the resonances of the b-$\vec{P}\vec{P}\underline{E}$* carbon. It is interesting to note that the spectrum of sample $E_9P_{26}E_9$ contains t-$\vec{P}\underline{\vec{P}}$* peaks with intensity approximately twice that of the b-$\vec{P}\underline{E}$* peaks. This observation is understandable in terms of relatively slow addition of the first E unit to the original PPO, followed by more rapid addition of subsequent E units. The fraction of P* end groups in sample $E_9P_{26}E_9$ was 0.2.

A number of other peaks associated with E* end groups occur in the region δ_C 68–71. These appear most clearly in the spectrum of sample $E_{0.3}P_{16}E_{0.3}$ shown in Figure 6c, where the assignments are made chiefly on the basis of correlation of peak intensities with the end group and tacticity distributions known from analysis of the terminal CH_2OH region and also by comparison of chemical shifts with those found for PEO homopolymer. These assignments are supported by the substituent shift calculations discussed below.

The main-chain carbon region of the spectrum of $E_9P_{26}E_9$ (Figure 7) is essentially the superposition of homopolymer spectra with the addition of peaks specific to the $\vec{P}$E junction. In the E CH_2 region (see Figure 7b) new peaks are observed at δ_C 70.60, 68.37, and 68.29, the last two together being equal in intensity to the first. The peak at δ_C 70.60 is assigned to the b-$\vec{P}\underline{E}$E carbon, and the remaining two to the a-$\vec{P}\underline{E}$E carbon split by stereoisomerism in the preceding $\vec{P}\vec{P}$ diad. The resonance of the t-$\vec{P}\underline{\vec{P}}$E carbon (see Figure 7a) proved more difficult to assign. When the resolution-enhanced CH subspectrum was examined the only peaks observed were intense peaks from $\vec{P}\underline{\vec{P}}\vec{P}$ triads and minor peaks corresponding in position and intensity to those arising from a-$\vec{P}\vec{P}$ initiation site (see the discussion the spectra of PPO homopolymer above). However, the two lowest frequency $\vec{P}\underline{\vec{P}}\vec{P}$ peaks were slightly more intense relative to the others than in PPO homopolymer or in PEP triblock copolymer, and it is tentatively proposed that the t-$\vec{P}\underline{\vec{P}}$E carbon gives two peaks (due to *m*/*r* isomerism) which fortuitously coincide with the two lowest frequency $\vec{P}\underline{\vec{P}}\vec{P}$ peaks. This assignment is strongly supported by the CH subspectrum of a random EP copolymer and by a semiempirical correlation of chemical shifts with methyl substituent position, both of which are discussed below.

EP Statistical Copolymers. Figure 8a shows the terminal carbon region of the spectrum of the low MW EP statistical copolymer CH-EP. Both t-$\vec{P}$* and b-$\underline{E}$* peaks are observed. Peaks occur at positions found in the spectra of the triblock copolymers and assigned to t-EE$\underline{\vec{P}}$* t-E$\vec{P}\underline{\vec{P}}$*, t-$\vec{P}\vec{P}\underline{\vec{P}}$*, b-EE$\underline{E}$*, b-$\vec{P}E\underline{E}$*, and b-$\vec{P}\vec{P}\underline{E}$* end triads. There is a more or less equal distribution of *m* and *r* $\vec{P}\vec{P}$ diads. There is no evidence of end groups other than E* or $\vec{P}$*, nor of initiation sites other than oxyethylene or oxypropylene. In this polymer two additional end units, E$\vec{P}$E* and $\vec{P}$E$\vec{P}$*, may occur. The resonances of the terminal carbons would be expected to be close to those of b-$\vec{P}\vec{P}\underline{E}$* and t-EE$\underline{\vec{P}}$*, respectively. In the case of the former, it is noticeable that whereas in the EPE triblock spectra, the b-$\vec{P}\vec{P}\underline{E}$* signal is a symmetrical doublet at δ_C 61.72 and 61.83, the corresponding peaks in the statistical copolymer are not of equal intensity, that at δ_C 61.72 being more intense. The additional component at this frequency is therefore tentatively assigned to a singlet from the b-E$\vec{P}\underline{E}$* carbon. The t-$\vec{P}$E$\underline{\vec{P}}$* and t-EE$\underline{\vec{P}}$* resonances are indistinguishable.

In discussing the main-chain resonances, whose CH and CH_2 subspectra are shown in Figures 8b and 9, respectively, it is convenient to follow Whipple and Green[1] in dividing the spectrum into four regions, I–IV, covering the

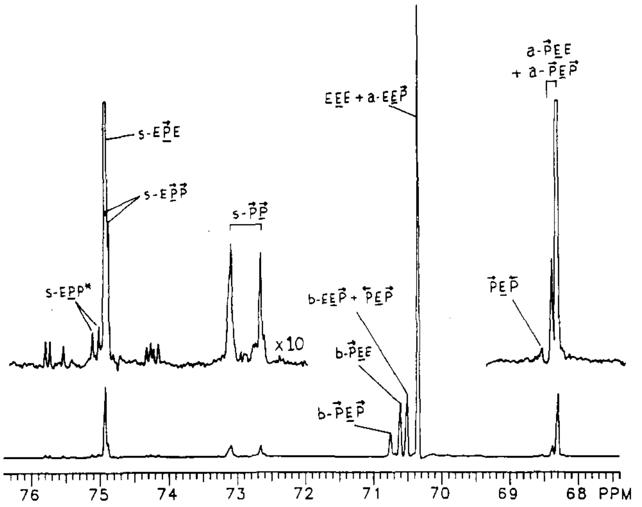

Figure 9. CH_2 subspectrum of low molecular weight statistical EP copolymer, CH-EP resolution-enhanced with $T_e = 0.2$ and $T_g = 0.3$ s.

ranges (in $CDCl_3$) δ_C 73.6–78, 71.8–73.6, 69.2–71.8, and 67.4–69.2, respectively.

Region III (see Figure 9) consists of four clearly resolved CH_2 peaks, of which three at δ_C 70.33, 70.50, and 70.60 can be assigned to (EE̲E + a-EE̲P⃗), (b-EE̲P⃗ + P⃖E̲P⃗), and b-P⃗E̲E carbons, respectively, from the previous discussions. The peak at δ_C 70.50 also incorporates signals from the b-P⃗E̲P* and a-P⃗P⃗E̲* carbons. The fourth peak at δ_C 70.74 was not observed in the spectra of the block copolymers and can be assigned to the b-P⃗E̲P⃗ carbon on the basis of its low intensity and a chemical shift consistent with methyl substituent effects.

Region IV (see Figure 9) consists principally of two CH_2 peaks at δ_C 68.37 and 68.29 of unequal intensity from a-P⃗E̲P⃗ and a-P⃗E̲E carbons. These should have the same chemical shift taking only methyl substituent effects into account. However, the spectra of the EPE triblock copolymers showed that the a-P⃗P⃗E̲E resonance is split evenly by *m*/*r* isomerism into lines at δ_C 68.37 and 68.29. In contrast, no splitting is expected for resonances of the a-EP⃗E̲P⃗ or a-EP⃗E̲E carbons. The region IV line at δ_C 68.37 therefore arises from *m* (or *r*) [a-P⃗P⃗E̲P⃗ + a-P⃗P⃗E̲E] carbons while the line at δ_C 68.29 arises from *r* (or *m*) [a-P⃗P⃗E̲P⃗ + a-P⃗P⃗E̲E] carbons together with a-EP⃗E̲P⃗ and a-EP⃗E̲E carbons. Region IV also contains a minor peak at δ_C 68.50 which is not observed in the block copolymers. Its chemical shift is consistent with assignment to a-P⃗E̲P⃖ triad.

Region II consists principally of resonances from s-P⃗P̲⃗ carbons together with any t-P̲⃗P̲⃖ carbons. The s-P⃗P̲⃗ signals (see Figure 9) are split by *m*/*r* isomerism as in the P homopolymer. Minor peaks from s-P⃗P̲⃗P⃗* carbons were also evident as in PPO, consistent with the observation of a significant number of P⃗P⃗P⃗* chain ends as discussed above. The CH subspectrum (see Figure 8b) shows that P⃗P⃖ diads constitute only a very small proportion of the total CH signal. The t-P̲⃗P̲⃖ carbons here give principally two lines of approximately equal intensity at δ_C 72.75 and 73.12, in contrast to the PPO homopolymer where a wider shift dispersion is observed. The reduced number of peaks in the statistical copolymer is probably due to the fact that the P⃗P⃖ diads occur mainly in EP⃗P⃖E tetrads, in which only a double *m*/*r* splitting occurs.

Region I is by far the most complex, consisting of significant CH and CH_2 signals. The CH subspectrum (see Figure 8b) is dominated by a singlet at δ_C 74.75 attributable mainly to t-EP̲⃗E carbons. There are also less intense lines at the frequencies assigned, from the homo- and copolymer analyses discussed above, to internal t-P⃗P̲⃗P⃗, t-EP̲⃗P⃗, and t-P⃗P̲⃗E carbons, together with minor peaks associated with P chain ends. Analysis of the intensities of the end-group resonances indicates that P⃗P⃗ diads are distributed approximately equally between *m* and *r*, as in PPO homopolymer. The t-EP̲⃗P⃗ carbon is therefore distinguishable by a distinct peak at δ_C 74.94 together with a peak of similar intensity obscured by the t-EP̲⃗E peak. The small peaks of equal intensity at δ_C 75.26 and 75.10 correlate with *mm* and *mr* (or *rm*) t-P⃗P̲⃗P⃗ resonances, respectively. The accompanying *rm* (or *mr*) and *rr* t-P⃗P̲⃗P⃗ resonances would be expected at δ_C 75.06 and 74.86, respectively, but the peaks observed at these frequencies are considerably more intense than if this was their sole origin. It is reasonable to suppose that the additional intensity arises from overlap with t-P⃗P̲⃗E carbons split by *m*/*r* isomerism, as suggested above in the discussion of EPE block copolymers. Analysis of the CH subspectrum is thus capable of yielding proportions of P⃗ centered triads, provided that the *m*/*r* distribution is known.

The CH_2 subspectrum of region I (see Figure 9) shows one intense peak and a number of minor peaks, those in the regions δ_C 74.1–74.4, 75.5–75.8, and 76.8 being associated with P* chain ends. The intense peak at δ_C 74.93 arises mainly from s-EP̲⃗E carbons. As deduced from the spectra of the PEP triblock copolymers, this peak also contains a smaller component which, together with the peak at δ_C 74.89, constitutes the signal from the s-EP̲⃗P⃗ carbon split by *m*/*r* isomerism. The two remaining minor peaks at δ_C 75.03 and 75.10 are consistent with resonances of s-P̲⃖P̲⃗ carbons. However neither the number of peaks nor the frequencies correspond to P⃖P⃖P⃗P⃗ tetrads from initiation sites or to P⃗P⃖P⃗ triads as were found in PPO. These peaks may arise from an s-EP̲⃖P⃗ carbon, but their intensity is also consistent with an s-EP̲⃗P⃗* carbon. These two peaks were essentially absent in the CH_2 subspectrum of the high MW statistical EP copolymer UCONA, which favors the latter assignment.

The spectra of the high MW copolymer UCONA showed essentially the same features as those of the low MW sample, allowing for the difference in overall composition and proportion of end groups. The chain ends were principally EEP⃗* and EEE*. The P⃗P⃖ content was effectively zero.

Table II summarizes the assignments for homopolymers and copolymers. These are consistent with earlier less detailed studies.[1-3]

It should be noted that the reported chemical shifts apply to solutions of the stated concentrations. For solutions of E_{39} and P_{26} containing 1 g of polymer/cm^3 of $CDCl_3$, the terminal-unit peaks moved to low frequency by up to 0.4 ppm and the $CDCl_3$ peak moved to high frequency by 1 ppm, relative to the main-chain peaks.

Chemical Shift Additivity Scheme. Whipple and Green[4] described qualitatively how the backbone ^{13}C spectra of statistical EP copolymers could be understood in terms of chemical shifts which depended on the distance of methyl groups from a particular carbon. Halmo et al.[3] developed a similar quantitative scheme for EP copolymers dissolved in C_6D_6, but full details of the assignment procedures were not given. We are able to establish such a scheme more firmly because of the use of block copolymers and CH/CH_2 subspectra to obtain unequivocal assignments and to extend the scheme to include end groups.

Table III
Comparison of Calculated and Experimental ^{13}C Chemical Shifts (δ) in EP Copolymers[a]

		chem shift	
carbon	substnt effects	calcd	exptl
b-$\vec{P}\underline{E}\vec{P}$	$\delta + \delta'$	70.77	70.74
$\overleftarrow{P}\underline{E}\vec{P}$	δ	70.50	70.50
$\vec{P}\underline{E}\overleftarrow{P}$	$\gamma + \delta'$	68.64	68.50
t-$E\underline{\vec{P}}E$	α	74.66	74.73
s-$E\underline{\vec{P}}E$	β	74.93	74.91
t-$E\underline{\vec{P}}\vec{P}$	$\alpha + \delta$	74.83	74.84
s-$E\underline{\vec{P}}\vec{P}$	β	74.93	74.89
t-$\vec{P}\underline{\vec{P}}E$	$\alpha + \delta'$	74.93	74.98
t-$\underline{\vec{P}\overleftarrow{P}}$	$\alpha + \gamma$	72.62	ca. 73.1
s-$\underline{\overleftarrow{P}\vec{P}}$	$\beta + \delta$	75.10	75.06
t-$E\underline{\vec{P}}$*	$\alpha + \alpha^*$	65.79	65.98
s-$E\underline{\vec{P}}$*	$\beta + \beta^*$	76.95	76.76
t-$\vec{P}\underline{\vec{P}}$*	$\alpha + \alpha^* + \delta'$	66.06	66.15
s-$\vec{P}\underline{\vec{P}}$*	$\beta + \beta^* + \gamma$	74.91	75.00
t-$E\underline{\vec{P}}\vec{P}$*	$\alpha + \delta + \delta^*$	74.59	75.06
t-$\vec{P}\underline{\vec{P}}\vec{P}$*	$\alpha + \delta + \delta' + \delta^*$	74.86	75.51
b-$\vec{P}\vec{P}\underline{E}$*	$\alpha^* + \delta'$	61.73	61.78
a-$\vec{P}\vec{P}\underline{E}$*	$\beta^* + \gamma$	70.31	70.49
b-$\vec{P}\underline{E}E$*	$\delta' + \delta^*$	70.36	70.51

[a] See text for values of substituent parameters.

We equate the chemical shift to the shift of the interior carbons of PEO, δ_C 70.33, plus corrections for the presence of methyl groups (α, β, γ, or δ) or hydroxy groups (α^*, β^*, or δ^*) relative to the carbon in question. In EP copolymers methyl groups of type α, β, or γ each have one type of interaction, viz., $\alpha \equiv \underline{C}CH_3$, $\beta \equiv \underline{C}CHCH_3$, and $\gamma \equiv \underline{C}OCHCH_3$. However, two δ interactions must be distinguished: $\delta \equiv \underline{C}OCH_2CHCH_3$ and $\delta' \equiv \underline{C}CH_2OCHCH_3$. The γ^*-OH placement does not occur. Stereoisomerism is not taken into account in the scheme: where peaks originating from different tacticities are observed, the mean chemical shift is used.

The following unequivocal assignments provide values of the methyl contributions: b-$E\underline{E}\vec{P}$, $\delta = 0.17$ ppm; b-$\vec{P}\underline{E}E$, $\delta' = 0.27$ ppm; a-$\vec{P}\underline{E}E$, $\gamma = -2.04$; t-$\vec{P}\underline{\vec{P}}\vec{P}$, $\alpha + \delta + \delta' = 4.77$ ppm, whence $\alpha = 4.33$ ppm; s-$\vec{P}\underline{\vec{P}}\vec{P}$, $\beta + \gamma = 2.56$ ppm, whence $\beta = 4.60$. For the hydroxy contributions, we used b-$EE\underline{E}$*, $\alpha^* = -8.87$; a-$EE\underline{E}$*, $\beta^* = +2.02$; b-$E\underline{E}E$*,, $\delta^* = -0.24$. The chemical shifts calculated for other sequences are compared with assigned values in Table III. The agreement is excellent except for the t-$\underline{\vec{P}\overleftarrow{P}}$, t-$E\underline{\vec{P}}\vec{P}$* and t-$\vec{P}\underline{\vec{P}}\vec{P}$* carbons, possibly due to unusual steric interactions in these sequences.

These shift contributions can be used as a guide to locating as yet undetected resonances associated with end groups. The a-$\vec{P}\underline{E}$* carbon is predicted to occur at δ_C 70.35, the b-$\vec{P}\underline{E}E$* at δ_C 70.36, and the b-$E\underline{E}\vec{P}$* at δ_C 70.26; all of these are obscured by the intense EEE peak. The b-$\vec{P}\underline{E}\vec{P}$* carbon is predicted to lie at δ_C 70.53, i.e., coincident with the b-$E\underline{E}\vec{P}$ peak.

Sequence Distribution in EP Statistical Copolymer. With the spectral interpretation described above, it is possible to analyze intensity data to obtain reasonably accurate estimates of the triad sequence distribution in EP copolymers. Table IV gives the distribution for the two commercial statistical copolymers. Strictly the proportions of EEE, $EE\vec{P}$, and $\overleftarrow{P}E\vec{P}$ triads cannot be individually determined, since the $E\underline{E}E$ and a-$E\underline{E}\vec{P}$ resonances overlap, as do the b-$E\underline{E}E$ and $\overleftarrow{P}\underline{E}\vec{P}$ resonances. The EEE and $EE\vec{P}$ proportions given in Table IV have been obtained by assuming that ($\overleftarrow{P}E\vec{P}$) is zero. This assumption is reasonable because of the low oxypropylene content of both CH-EP and UCONA. No information is available concerning the initiation or reaction conditions, and it is not possible to use these data to evaluate reactivity ratios, but the measured distribution can be tested for consistency against necessary statistical relationships.

Table IV
Triad Proportions in Commercial EP Statistical Copolymers[a]

	polymer	
triad	CH-EP	UCONA
EEE	0.335	0.478
$EE\vec{P}$	0.130	0.136
$\vec{P}EE$	0.113	0.131
$\vec{P}E\vec{P}$	0.071	0.039
$\vec{P}E\overleftarrow{P}$	0.003	0.002
$\vec{P}\vec{P}\vec{P}$	0.059	0.008
$E\vec{P}\vec{P}$	0.080	0.033
$\vec{P}\vec{P}E$	0.043	0.033
$E\vec{P}E$	0.120	0.138
$E\vec{P}\overleftarrow{P}$	0.011	
EEE*	0.001	0.001
$\vec{P}EE$*	0.001	
$E\vec{P}E$*	0.001	
$\vec{P}\vec{P}E$*	0.002	
$\vec{P}\vec{P}\vec{P}$*	0.014	
$E\vec{P}\vec{P}$*	0.007	
$\vec{P}E\vec{P}$* + $EE\vec{P}$*	0.009	0.001

[a] Uncertainties are ca. ±5%.

For an infinite chain with only H→T addition of P units, the following relationships are necessarily obeyed

$$(\vec{P}EE) = (EE\vec{P}) \qquad (1)$$

$$(\vec{P}\vec{P}E) = (E\vec{P}\vec{P}) \qquad (2)$$

$$(EE\vec{P}) + (\vec{P}EE) + 2(\vec{P}E\vec{P}) = (E\vec{P}\vec{P}) + (\vec{P}\vec{P}E) + 2(E\vec{P}E) \qquad (3)$$

For the high MW sample, the values of the left- and right-hand sides of eq 1–3 are respectively 0.131 vs 0.136, 0.033 vs 0.033, and 0.345 vs 0.342, in excellent conformity with statistical requirements. For the low MW sample, resonances due to both chain ends and inverted P units are detected, and the necessary statistical relationships are (for oxyethylene or oxypropylene initiation sites)

$$(E\vec{P}\vec{P}) + (\overleftarrow{P}\vec{P}\vec{P}) = (\vec{P}\vec{P}E) + (\vec{P}\vec{P}\overleftarrow{P}) + (\vec{P}\vec{P}E^*) + (\vec{P}\vec{P}\vec{P}^*) \qquad (4)$$

$$(EE\vec{P}) + (\vec{P}E\vec{P}) + 2(\overleftarrow{P}E\vec{P}) = (E\vec{P}E) + (E\vec{P}\vec{P}) + (E\vec{P}\overleftarrow{P}) + (E\vec{P}E^*) + (E\vec{P}\vec{P}^*) \qquad (5)$$

$$(\vec{P}EE) + (\vec{P}E\vec{P}) + 2(\vec{P}E\overleftarrow{P}) + (\vec{P}EE^*) + (\vec{P}E\vec{P}^*) = (E\vec{P}E) + (\vec{P}\vec{P}E) + (E\vec{P}\overleftarrow{P}) \qquad (6)$$

(These equations ignore end triads containing inverted P units.) Some of the triads involved here such as ($\overleftarrow{P}\vec{P}\vec{P}$) and ($\vec{P}\vec{P}\overleftarrow{P}$) have not been determined, but these are of very low intensity. Ignoring these, the values of the left- and right-hand sides of eq 4–6 are, respectively, 0.08 vs 0.06, 0.20 vs 0.22, and 0.19 vs 0.16. Allowing for cummulative errors in combining numerous independent measurements, the agreement with statistical requirements is satisfactory.

From a diad analysis, Whipple and Green[1] showed that for an infinite chain with peak assignments identical with those given here, the intensities of regions I, II, and IV should obey eq 7. Defining A_x as the fractional contributions of region x to the total intensity, the high MW sample yields $A_I = 0.189$, $A_{II} = 0.024$, and $A_{IV} = 0.083$. Hence $A_I - A_{II} - 2A_{IV} = -0.001$, in excellent agreement with the statistical expectations. In fact Whipple and Green[1]

$$A_I - A_{II} - 2A_{IV} = 0 \qquad (7)$$

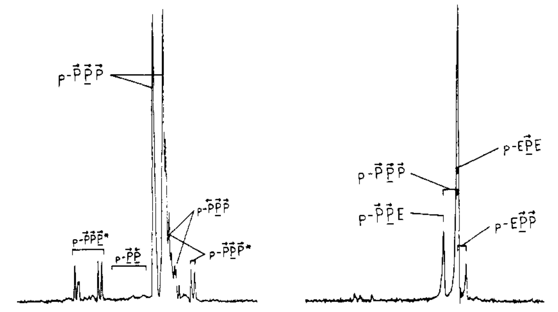

Figure 10. Resolution-enhanced CH_3 spectra: (a) P_{26}, $T_e = 0.25$ and $T_g = 0.55$ s (a one-carbon resonance, probably p-P$\underline{\vec{P}}\vec{P}\vec{P}$*, is obscured by the intense peak at δ_C 17.18 (see text)); (b) high molecular weight statistical copolymer UCONA ($T_e = 0.2$ and $T_g = 0.5$ s).

found that for their samples, eq 7 was not obeyed, the left-hand side amounting systematically to some 5% of the total intensity. Two explanations were suggested. The first was that their assignment of "hidden" peaks, in particular that of t-$\vec{P}\overleftarrow{P}$ carbons to region II, was incorrect. However, the CH subspectra shown here demonstrate that this assignment was correct. Their second explanation was that end groups were not negligible, and this appears to be the true reason. This study has shown that numerous CH and CH_2 resonances associated with end groups contribute to region I, whereas regions II and IV are entirely main chain. For our low MW sample, the intensities are $A_I = 0.266$, $A_{II} = 0.062$, and $A_{IV} = 0.085$, giving $A_I - A_{II} - 2A_{IV} = 0.034$. If the penultimate carbon signals are subtracted from region I, we obtain $A_I - A_{II} - 2A_{IV} = 0.01$, which is within experimental error of the expected zero value.

Methyl Resonances. In principle, the dependence of the CH_3 signals on stereochemistry and sequence structure should be analogous to that of the CH signals. However, the sensitivity of the CH_3 chemical shift to these factors was found to be much less than that of the CH chemical shift, with the result that the resolution of signals from different sequences was much worse in the CH_3 spectrum. Nevertheless we present a brief discussion of our results, both as a matter of record and for comparison with spectra obtained elsewhere under different conditions.

The spectra shown in Figure 10 demonstrate the dependence of the CH_3 resonances on stereochemistry and end group in PPO homopolymer and on stereochemistry and sequence structure in the high MW statistical EP copolymer.

In the spectrum of homopolymer P_{26}, Figure 10a, the peaks associated with terminal units were assigned on the basis of the dependence of their intensity on molecular weight (making use of the spectra of other homopolymers) and by comparison with the spectra of $E_9P_{26}E_9$ block copolymer. The p-$\vec{P}\vec{P}\underline{\vec{P}}$* and p-$\vec{P}\underline{\vec{P}}\vec{P}$* resonances are clearly distinguishable, as are the p-$\overleftarrow{P}\underline{\vec{P}}\vec{P}$ initiation-site resonances. The main-chain p-$\vec{P}\underline{\vec{P}}\vec{P}$ resonance consists of a doublet at δ_C 17.30 and 17.18. However, in order to explain the relative intensities of terminal-carbon resonances and of the two intense absorption regions at δ_C 17.3 and 16.9–17.2, it is necessary to assign one further CH_3 signal to the peak at δ_C 17.18. This hidden signal would presumably be either the p-$\vec{P}\underline{\vec{P}}\vec{P}\vec{P}$* or the p-$\overleftarrow{P}\vec{P}\underline{\vec{P}}\vec{P}$ resonance, most probably the former, because of the greater influence of the OH end group on the chemical shift. The p-$\underline{\vec{P}\overleftarrow{P}}$ peaks were assigned on the basis of the correspondence of their intensities with those of the t-$\underline{\vec{P}\overleftarrow{P}}$ peaks in the CH subspectrum (Figure 2a). These assignments agree qualitatively with those given in ref 14 for C_6D_6 solutions of PPO. A major difference is that here the main-chain resonances show only doublet stereochemical splitting, whereas in C_6D_6 the CH_3 shows[14] a quartet splitting similar to that of the CH peak. Evidently in $CDCl_3$ the p-$\vec{P}\underline{\vec{P}}\vec{P}$ chemical shift responds to the stereochemistry in only one direction along the chain (i.e. *m* or *r* splitting by either the preceding or the succeeding diad) whereas in C_6D_6 it responds to stereochemistry in both directions (i.e. *mm*, *mr*, *rm*, and *rr* splitting).

The CH_3 spectrum of the high MW statistical copolymer, Figure 10b, shows only three peaks. The assignments were based on comparison with the spectra of the triblock copolymer and on comparison of the relative intensities of the three peaks with those predicted from the triad statistics in Table IV. Taking the three peaks in order, from high to low frequency, the intensities as a fraction of the total methyl intensity are 0.20, 0.74, and 0.06 (observed) compared with 0.175, 0.747, and 0.078 (calculated). It is noteworthy that the p-$\vec{P}\underline{\vec{P}}$E peak shows no stereochemical splitting whereas the p-E$\underline{\vec{P}}\vec{P}$ peak does. This shows that the CH_3 resonance is affected by the stereochemistry of the succeeding diad.

Acknowledgment. The British Council provided financial assistance to Y.Z.L. and J.F.D.

Registry No. PE (block copolymer), 106392-12-5; EP, 9003-11-6.

References and Notes

(1) Whipple, E. B.; Green, P. J. *Macromolecules* **1973**, *6*, 38.
(2) Chen, X.-C. *Bopoxue Zazhi* **1984**, *1*, 409.
(3) Halmo, F.; Malik, L.; Liptaj, T. *Chem. Prum.* **1986**, *36*, 203.
(4) Rubenstein, D. L.; Nakashima, T. T. *Anal. Chem.* **1979**, *51*, 14651A.
(5) Lecocq, C.; Lallemand, J.-Y. *J. Chem. Soc., Chem. Commun.* **1981**, 150.
(6) Patt, S. L.; Shoolery, J. N. *J. Magn. Reson.* **1982**, *46*, 535.
(7) Ferrige, A. G.; Lindon, J. C. *J. Magn. Reson.* **1978**, *31*, 337.
(8) Doddrell, D. M.; Pegg, D. T.; Bendall, M. R. *J. Chem. Phys.* **1982**, *77*, 2745.
(9) Viras, F.; Luo, Y.-Z.; Viras, K.; Mobbs, R. H.; King, T. A.; Booth, C. *Makromol. Chem.*, in press.
(10) Holmes, B. S.; Moniz, W. B. *Polym. Prepr.* (*Am. Chem. Soc., Div. Polym. Chem.*) **1979**, *20*(2), 389.
(11) Schaefer, J. *Macromolecules* **1969**, *2*, 533; **1972**, *5*, 590.
(12) Oguni, N.; Shinohara, S.; Lee, K. *Polymer J.* **1979**, *11*, 755.
(13) Rabagliati, F. M.; Lopez, F. *Makromol. Chem., Rapid Commun.* **1985**, *6*, 141.
(14) Schilling, F. C.; Tonelli, A. E. *Macromolecules* **1986**, *19*, 1337.
(15) Wehrli, F. W.; Wirthlin, T. *Interpretation of Carbon-13 NMR Spectra*; Heyden and Son Ltd.: London, 1976; p 37.